FEATURE ARTICLE

ChemComm
www.rsc.org/chemcomm

Rational design of porous titanophosphates

Christian Serre,*[a] Francis Taulelle[b] and Gérard Ferey[a]

[a] *Institut Lavoisier, UMR CNRS 8637, Université de Versailles St-Quentin-en-Yvelines, 45 Avenue des Etats-Unis, 78035 Versailles Cedex, France. E-mail: serre@chimie.uvsq.fr; ferey@chimie.uvsq.fr; Fax: (1) 39 25 43 58; Tel: (1) 39 25 43 05*

[b] *RMN et Chimie du Solide, UMR CNRS 7140, Université Louis Pasteur, 4 Rue Blaise Pascal, 67070 Strasbourg, France. E-mail: taulelle@chimie.u-strasbg.fr*

Received (in Cambridge, UK) 29th April 2003, Accepted 29th July 2003
First published as an Advance Article on the web 28th August 2003

To rationally design new nanoporous materials based on titanophosphates, a small library of titanium phosphate crystalline nanoporous compounds has been build up and its compounds have been investigated by X-ray diffraction and by *in-* and *ex-situ* NMR. The main trends of the unusual titanium solution chemistry, of the prenucleation building units and of their assembling have been established. The classical trial and error strategy can therefore be replaced by a better control of the steps leading to the final targeted network.

1 Introduction

Microporous materials are very attractive solids because of the wide range of their applications in catalysis, shape-selective absorption, non linear optical (NLO) devices or molecular-based magnetism.[1–3] If the first discovered microporous solids were zeolites (aluminosilicates) and then aluminophosphates (AlPOs), elaborating porous compounds based on transition metals oxides or phosphates, is important for many applications.[1] Among them, titanium is a good candidate because of its photocatalytic activity and redox properties. Several titanium-based solids have found applications to date, such as the layered αTiP,[4] γTiP,[5] or dense KTP[6] titanophosphates or the $M_2Ti_2(PO_4)_3$ compounds (M = Li, Na…),[7] which exhibit applications in ion conductivity, ion exchange and non-linear optics. Some of the microporous titano-silicates (ETS-n) are also used as oxidation catalysts.[8–10] Since the discovery of MCM-41,[11] an analogue of mesoporous titanium dioxide, phosphate or silicate compounds would be of central importance for its applications in acid, redox catalysis or photocatalytic processes.[12,13]

The chemistry of titanium in water is limited by its very low solubility at almost all pH.[14] Titanium is only soluble to some extent in strongly acidic medium.[15,16] It is the main trend of titanium chemistry. It imposes to work at very low pH to observe soluble species. This is why the alternative route to get soluble species, by "chimie-douce", uses organic solvents and strong chelating agents.[15,17,18] This allows a delicate control of the condensation of titanium and has led to the synthesis and characterisation of a wide range of titanium alcoxo-clusters.[17] However, this alternative is limited for industrial processes by the expensive reagents. A need for synthetic strategies in water exists.

Besides, understanding of formation mechanisms of the nanoporous materials can be followed, as it has already been demonstrated on an oxyfluorinated microporous aluminophosphate, $AlPO_4$-CJ2, by *in situ* NMR and *ex situ* investigation.[19–21] The dynamics of the different steps of the synthesis as well as the formation of the chemical bonds can be observed, allowing characterisation of the Pre-Nucleation Building Units (PNBU) involved during the synthesis.

In addition, in our group, many hydrothermal syntheses and structure determination of organically templated oxyfluorinated metalophosphates with an open structure based on p-elements (Al, Ga) and transition metals (Fe, V…) have been carried out.[22,23]

Finally, to gain some control on titanium systems, we use a three-step strategy. Firstly, a study of titanium phosphates under hydrothermal conditions is undertaken to discover the possible topological arrangements. Secondly, an NMR study of the titanium fluorophosphates aqueous solutions allows identification of the species in solution. The elucidation of the PNBU is performed by NMR *in situ* and *ex situ* analyses of crystallisation. In a last step, rational design is successfully applied to the synthesis of a mesostructured titanium phosphate. The results presented here constitute the body of knowledge necessary to undertake and develop rational syntheses of titanium-based nanoporous materials.

2 Hydrothermal synthesis of titanium-based solids

Within the past decades, most of the titanium phosphates (αTiP, γTiP) synthesised under hydrothermal conditions exhibit lamellar structures.[4–6] It is only recently that Poojary *et al.* reported the first three-dimensional titanium phosphates with an open structure.[24] Sevov *et al.* also characterized templated mixed valence three-dimensional titanium phosphates.[25,26] Meanwhile, our group has initiated a systematic study of rational design of titanium phosphates, fluorophosphates and diphosphonates. Synthesis parameters such as stoichiometry, P : Ti and F : Ti ratios, pH, synthesis time, temperature and nature of the inorganic precursors or organic templates were investigated. Several solids, exhibiting various dimensionalities and compositions, were characterised using single crystal or powder X-ray diffraction (see Table 1). Microporous,[27,28] pillared,[29] layered and oxyfluorinated[30,31] or mixed valence solids[32] were obtained. Recently, new templated titanium phosphates synthesised either in non-aqueous media or using titanium metal as a precursor, have also been reported.[33–35] Among them, two are three-dimensional with an open structure. The available data for hydrothermal syntheses are updated in Table 1.

Though the number of characterised solids is still limited, about 30 structures known, it is yet possible to suggest a classification of results as a function of the several synthetic parameters. Two main parameters appear at the forefront: the acidity and the competitive complexation of titanium by fluorine and phosphate.

2.1 Influence of the acidity

The inventory of the structures of titanium phosphates or diphosphonates, characterised in this work, suggests a clear correlation between the pH and the dimensionality of the

DOI: 10.1039/b304703b

Table 1 Characterised titanium phosphates or diphosphonates synthesised under hydrothermal conditions

Compound	Titanium precursor	Complexing acid	Organic template	Conditions	Network dimensionality
αTiP[4]	$TiCl_4$	H_3PO_4	—	180 °C, 3 d	2D
γTiP[5]	$TiCl_4$	H_3PO_4	—	180 °C, 3 d	2D
NH_4TP[a]	$TiCl_4$	H_3PO_4	NH_3	180 °C, 3 d	3D
γTiP, en or MIL-44[36]	$TiO_2{\cdot}H_2O$	H_3PO_4	en	180 °C, 3 d	2D
$Ti_3(PO_4)_4(H_2O)_2{\cdot}NH_3$[24]	$TiCl_3$	H_3PO_4	NH_3	190 °C, 5 d	3D
$Ti_2O(PO_4)_2{\cdot}2H_2O$ or ρTiP[24]	$TiCl_4$	H_3PO_4	—	190 °C, 5 d	3D
$NH_4{\cdot}Ti_2O_3(HPO_4)_2(PO_4)_2$[24]	$TiCl_4$	H_3PO_4	NH_3	190 °C, 5 d	3D
$Ti^{III}Ti^{IV}(PO_4)(HPO_4)_2{\cdot}(NH_2{-}(CH_2)_3{-}NH_2)_{0.5}.2H_2O$[25]	Ti (metal)	H_3PO_4, H_3BO_3	1,3-Dap	200 °C, 3 d	3D
$Ti^{III}Ti^{IV}(HPO_4)_4.(NH_2{-}(CH_2)_2{-}NH_3){\cdot}H_2O$[26]	Ti (metal)	H_3PO_4, H_3BO_3	en	200 °C, 3 d	3D
$Ti_2(PO_4)_2F_4$, $N_2C_nH_{10}$ or MIL-6$_n$ (n = 2, 3)[30]	$TiO_2{\cdot}H_2O$	H_3PO_4, HF	en, 1,3-Dap	180 °C, 3 d	2D
$Ti^{III}Ti^{IV}F(PO_4)_2.2H_2O$ or MIL-15[32]	$TiCl_3$	H_3PO_4, HF	Dabco	210 °C, 3 d	3D
$Ti_6O_3(H_2O)_3(PO_4)_7{\cdot}(H_3O){\cdot}H_2O$ or MIL-18[27]	$TiO_2{\cdot}H_2O$	H_3PO_4, HF	1,3-Dap	190 °C, 3 d	3D
$[Ti_3O_2(OH)_2(HPO_4)_2(PO_4)_2].(NH_3{-}(CH_2)_3{-}NH_3)_2{\cdot}(H_2O)_2$) or MIL-28$_3$[31]	$TiO_2{\cdot}H_2O$	H_3PO_4, HF	1,3-Dap	180 °C, 3 d	2D
$[Ti_3O_2(H_2PO_4)(HPO_4)_{3.5}(PO_4)_2]{\cdot}(NH_3{-}(CH_2)_2{-}NH_3)_2$[33]	Ti (metal)	H_3PO_4	en	240 °C, 5 d	3D
$[Ti_2(H_2PO_4)_2(HPO_4)_2]{\cdot}(NH_3{-}(CH_2)_2{-}NH_3)_2$[33]	Ti (metal)	H_3PO_4	en	240 °C, 5 d	3D
$[Ti_7(HPO_4)_6(PO_4)_6]{\cdot}(NH_3{-}(CH_2)_3{-}NH_3)_2$[33]	Ti (metal)	H_3PO_4	1,3-Dap	240 °C, 5 d	3D
$TiO(O_3P{-}(CH_2){-}PO_3)$, $(NH_4)_2$ or MIL-10[37]	$TiO_2{\cdot}H_2O$	$H_3O_2P{-}CH_2{-}PO_3H_2$	NH_3	180 °C, 3 d	1D
$Ti_3O_2(H_2O)_2(O_3P{-}(CH_2){-}PO_3)_2$, $(H_2O)_2$ or MIL-22[28]	$TiO_2{\cdot}H_2O$	$H_3O_2P{-}CH_2{-}PO_3H_2$	—	210 °C, 3 d	3D
$Ti(O_2P{-}(CH_2)n{-}PO_3)$ or MIL-25n (n = 2, 3)[29]	$TiO_2{\cdot}H_2O$	$H_3O_2P{-}(CH_2)_n{-}PO_3H_2$ (n = 2, 3)	NH_3	190 °C, 3 d	3D

en = ethylenediamine; dap = 1,3-diaminopropane; dabco = 4,4-diazabicyclooctane.[a] NH_4TP is isostructural with KTP.[6]

framework (Fig. 1). Titanium goes from "isolated" titanium octahedra or clusters, linking two to three octahedra, to eventually chains of octahedra.

Though acidity and complexant role can not be separated, the source of acidity, H_3PO_4 or HF, being also the source of complexant, we will try to disentangle both aspects. Rationalising syntheses imposes to define a strict order for reactant addition. In our protocols, this order is, the source of titanium, the solvent, H_3PO_4 and/or HF and finally, after having produced sometimes a clear solution, the amine followed by hydrothermal treatment.

The speciation of titanium in solution depends on several factors, $[H_2O]/Ti$, $[H_3PO_4]/Ti$ and $[HF]/Ti$ as well as pH. Actually, the last parameters may be deduced by the relative amount of acids to the added amine. The acidity is measured at two stages, before addition of amine and at the end of synthesis. The first pH lies between 0 to 3. After addition of the amine and reaction, the final pH ranges between 0 to 8.

In all these syntheses, the coordination state of titanium remains six. Therefore, controlling the formation of the network means controlling, as the first stage, the environment of titanium. It will contain, H_2O, H_3PO_4 and HF depending on composition ratios, and the actual charge of the species will depend on deprotonation of each ligand, H_2O, H_3PO_4 and HF.

Acidity controls the state of deprotonation of the different kinds of species that form in solution containing all the solvent of the ligands. First, the fully hydrated titanium, $Ti(H_2O)_6^{4+}$ must be considered, then $Ti(H_3PO_4)_x(H_2O)_{6-x}^{4+}$, $Ti(HF)_x(H_2O)_{6-x}^{4+}$ and eventually $Ti(HF)_x(H_3PO_4)_y(H_2O)_{6-x-y}^{4+}$ and their phosphonate equivalents. As pH increases from 0, the titanium complex loses its protons and therefore is prone to condense. Using the partial charge method,[14,38] one can show that, at pH = 0, $Ti(H_2O)_6^{4+}$ has already lost two protons and exists in both forms: $TiO(H_2O)_5^{2+}$ or $Ti(OH)_2(H_2O)_4^{2+}$. The existence of this titanyl bond has been investigated and it has

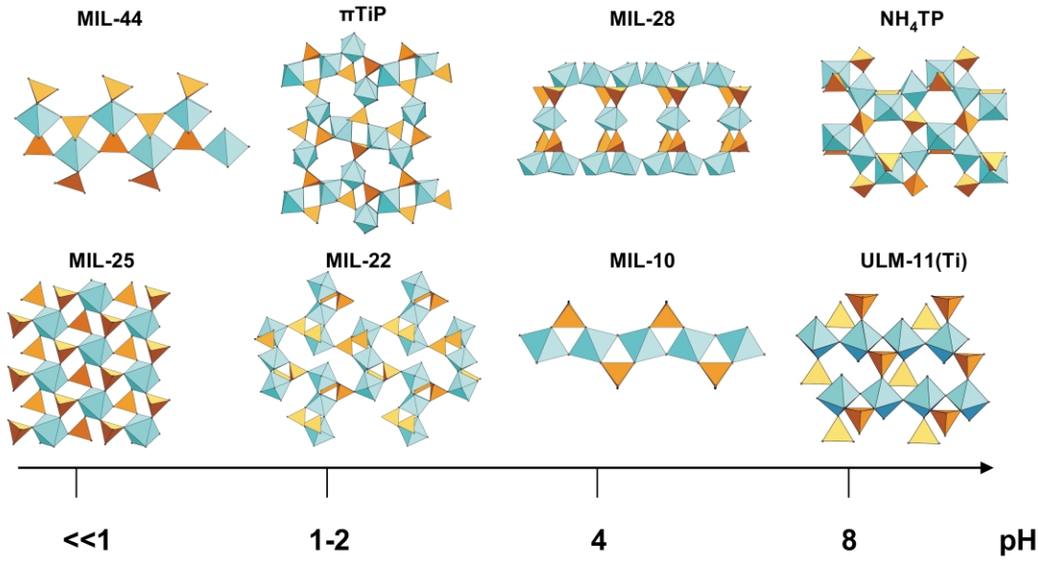

Fig. 1 Inorganic networks of some titanium-based solids obtained under hydrothermal conditions as a function of the final pH. Solids are reported depending on the titanium octahedra connection mode (monomers, dimers, trimers, chains).

been shown that the two forms with titanyl TiO and $Ti(OH)_2$ interconvert in water (Fig. 2).[39] The presence of phosphate and

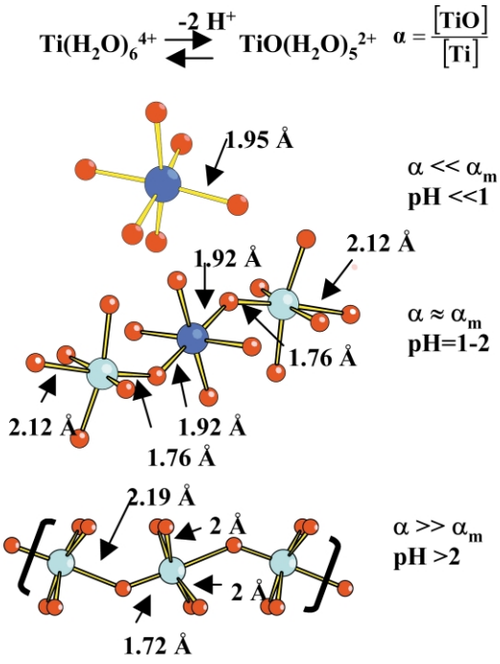

Fig. 2 Connection mode of clusters of titanium octahedra present within titanium phosphate or diphosphonate obtained under hydrothermal conditions. Distorted and regular titanium atoms are in cyan or blue, respectively while oxygen atoms are in red.

fluorine in the complexation sphere of titanium modifies this equilibrium, as calculated by Pacha.[40] Even at pH = 0, fluoride bonds to titanium without being protonated, $Ti(F)_x(H_2O)_{6-x}^{4-x}$ or $Ti(F)_x(H_3PO_4)_y(H_2O)_{6-x-y}^{4-x}$ have already lost two protons as the non complexed titanium, though $Ti(H_3PO_4)_x(H_2O)_{6-x}^{4+}$ is still fully protonated. Fluorine stabilises the titanyl bond at pH = 0, and $TiOF(H_2O)^{4+}$ depresses the amounts of other $TiF_x^{(4-x)+}$ complexes, with x = 2,3 and 4.[41] When fluorides are in excess, TiF_5^- and TiF_6^{2-} are formed. When considering the fluorophosphate species, progressive substitution of water by phosphates in the coordination sphere of Ti takes place, and the fluorophosphate species behave more or less like the fluoride case. So, it is only with $Ti(H_3PO_4)_x(H_2O)_{6-x}^{4+}$ that the coordination sphere is fully protonated and can be progressively deprotonated.

Two types of condensation may occur, condensation through the complexant, fluoride or phosphate, or through OH. The latter case proceeds in two steps, a fast hydroxylation followed by proton loss, leading to Ti–O–Ti bonds, as described by Henry's calculations.[14] No Ti–OH–Ti bridges are therefore observed, only Ti–O–Ti bonds, with corner-sharing connection between TiO_6 octahedra. The presence of Ti–O–Ti bridges with a titanyl bond indicates that deprotonation has taken place at condensation stage.

In solution without fluorides, under very acidic conditions, $Ti(H_3PO_4)_{6-x}(H_2O)_x^{4+}$ would be the main complex in solution. Deprotonation affects first the phosphate instead of the solvating water, leading to condensation through phosphate bridges. Regular titanium octahedra surrounded by phosphates and water are expected, leading to condensation to TiO_6 in the crystal connected only to phosphate groups. The dimensionality of the crystal is therefore only related to the protonation of the phosphate group. A $P(OTi)_3(OH)$ limits the dimensionality to lamellar compounds like α or γ TiP.

When the acidity decreases (pH = 1–2), the amount of $Ti(OH)(H_2O)_5^{3+}$, $TiO(H_2O)_5^{2+}$ or $Ti(OH)_2(H_2O)_4^{2+}$ or their equivalent fluorinated fluorophosphated forms, increase at the expense of the fully protonated species. Condensation of TiO_6 octahedra occurs through formation of a Ti–O–Ti bond. These clusters contain therefore regular and distorted TiO_6. At higher pH (> 2), only TiO_6 containing titanyl species are present, in clusters or in chains.[39,42]

A further increase of pH without either HF or H_3PO_4 would favour clusters of growing size, and eventually lead to hydrated titanium dioxide $TiO_2{\cdot}nH_2O$.[41,43]

2.2 Competitive complexation fluorine/phosphates

The titanium coordination sphere contains H_2O, HF or H_3PO_4 or their deprotonated forms. The order of group electronegativity in acidic media where all species are fully protonated is H_2O < H_3PO_4 < HF. HF or H_3PO_4 compete easily with water, and the coordination sphere contains H_2O, F^- or H_3PO_4 in proportions fixed by the composition. H_3PO_4 buffers the deprotonation of the titanium complex, while F^- maintains the global acidity of titanium even in the presence of H_3PO_4. It allows therefore formation of a Ti(OH) or a titanyl bond at quite low pH. However, with Ti(IV), F^- does not lead to TiF bridges. Therefore it inhibits the network formation. It is only with Ti(III) that we obtained Ti–F–Ti bridges in full analogy with their trivalent metal behaviour (Al, Ga). The organic ammonium stabilises fluorine linked to titanium(IV) in terminal positions. When using ethylenediamine as the template in a highly fluorinated synthesis medium (see Fig. 3), no solid ever

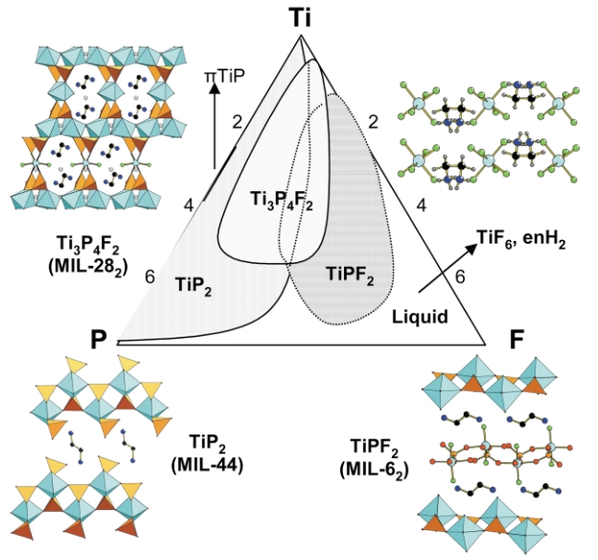

Fig. 3 Qualitative ternary diagram (Ti, F, P) of the titanium system under hydrothermal conditions using ethylenediamine. Titanium, phosphorus, fluorine, carbon and nitrogen atoms are in cyan, orange, green, black and deep blue respectively.

crystallizes in hydrothermal conditions and evaporating the liquid gives crystals of isolated TiF_6^{2-} complexes whose charge is compensated by the organic cation. Fluorides plays the role of a protecting group, when kept in the coordination sphere of titanium. It permits, however, in the presence of H_3PO_4, the formation of Ti–O–Ti bridges, that would be otherwise inhibited by using H_3PO_4 only. However, when the Ti–O–Ti bonds are formed, fluorides can be removed by a high phosphate content. Even in the presence of fluorine, one can produce a layered titanium phosphate with a P : Ti ratio of 2 (γ-TiP-en). Between these two cases, oxyfluorinated titanium phosphates are formed with fluorine atoms present only in a terminal position. In both cases, organic diamines are interacting with terminal P–OH or Ti–F groups to ensure the stability of the structure. These results, despite the small number of solids

characterised up to now, indicate the existence of a competitive complexation phenomenon of titanium by phosphate groups and fluorine atoms. In the absence of an organic template, no fluorinated solid has been isolated; this comes from the difference of behaviour between fluorine and phosphates; if their complexing force seems comparable under acidic conditions in water, fluorine does not possess the strong bridging capacity of the phosphates for titanium(IV) atoms. NMR studies indicate that when the resulting solid is phosphated and non-fluorinated, the residual species present in solution are highly fluorinated titanium fluoride or fluorophosphates.[41]

The first pH governs the hydrolysis ratio of titanium, and therefore the degree of connectivity of the titanium sub-lattice framework (Figs. 1, 2). The final pH controls the phosphate groups connectivity. This provides several types of Secondary Building Units (SBU) for the titanium phosphate or diphosphonate system under hydrothermal conditions. Octahedral titanium and tetrahedral PO_4 for phosphates (or PO_3C for phosphonates) with Ti–O–P and Ti–O–Ti connections are present. It leads to mono, di, trimeric units or chains of titanium octahedra grafted by phosphate or diphosphonate groups.

When the pH increases, TiO_6 polyhedra start to be connected by vertices, in clusters or at higher pH, in chains.

2.3 Conclusion

The first mixture of titanium source, solvent, HF and H_3PO_4, produces a solution containing Ti surrounded by H_2O, F^- and H_3PO_4. Without fluorides, at pH between 2 and 3, H_3PO_4 starts to deprotonate, Ti–O–P bonds form. In the presence of F^-, Ti containing species have already lost 2 protons and form a titanyl bond. Depending on F : P ratio, the fluorides may or may not stay in the crystal, and if they stay inside, they decrease the titanium functionality being terminal TiF. Adding an amine and proceeding with hydrothermal treatment leads to further deprotonation of phosphates, which therefore connect the network. The first pH controls the number of Ti–O–Ti bridges, non-connecting bonds, the F/P the number of "protected" Ti vertices, and the vertices remaining define the node functionality of each titanium. As the amount of amine defines the final pH, *i.e.* the protonation state of the phosphate, it defines the dimensionality of the network. Hydrolysis ratio of titanium, functionality control by F/P, dimensionality control by final pH and pore shape by amine selection, allow to rationally design the porous titanophosphates. Diphosphonates share the main features of the phosphate case.

3 Mechanism of formation

Compounds such as zeolites are widely used as catalysts or adsorbents, but little is known about their crystallisation mechanisms and there is still a need for understanding them.[44] Collecting crystallochemical results on titanium fluorophosphates was the first part of this project, the next step was the NMR study of the relation between processes occurring within the solution and the formation of the solid.

Various techniques are used to study the crystallisation of microporous solids. As two main techniques were extensively used in this study, X-ray diffraction and *in situ* NMR, a brief description of them is provided.

3.1 X-Ray diffraction experiments

A comprehensive review on the use of *in situ* X-ray diffraction as a tool to characterise the mechanisms of formation of crystal has been published.[45] Therefore, only a very short presentation of this technique is given below. Using either laboratory or high energy X-ray synchrotron sources, these experiments are designed to elucidate the formation of inorganic crystals in order to achieve a rational design of such solids. By using reaction cells for *in situ* powder diffraction studies, information such as the course of the reaction, the phase identification as well as quantitative kinetics information are acquired. *In situ* diffraction using neutron sources and combination of X-ray synchrotron and spectroscopic techniques (EXAFS) are also alternatives.

Many types of inorganic materials such as zeolites, metal-substituted alumino-phosphates, open-framework gallium phosphates, oxides and even mesoporous solids (MCM-41) can be studied using *in situ* diffraction. However, the main drawback of *in situ* XRD is that only crystallisation is studied and no information on either the species in the solution or on the process between the solid and liquid phases is given. This is one of the major reasons why *in situ* NMR technique was developed.

3.2 *In/Ex situ* NMR

3.2.1 Methodology. This methodology develops in three steps. First, identification of the primary building units (PBU), *i.e.* fluorophosphate titanium complexes present in solution, at room temperature, is carried by NMR.[42] These species are useful representatives of the PBU during hydrothermal synthesis of nanoporous and mesoporous materials. Second, an *in situ* NMR study of the formation of the solid allows observing the signals of the Pre-Nucleation-Building-Units (PNBU) which is the bottleneck of crystallisation. Third, the *ex situ* study consists of separating the solid from the liquid phase at different steps of the synthesis and analysing them using different techniques such as quantitative analysis, XRD, solid state NMR (solid) and liquid NMR (liquid). This method was applied successfully to the study of the mechanism of formation of the oxyfluorinated aluminium phosphate $AlPO_4$-CJ2 whereas a four ring (4R) unit was identified as the PNBU responsible of the crystallisation of the solid.[19–21] During the course of this study, it appeared clearly that PNBU may differ from SBU, which are the structural units, by an isomerisation in SBU to adapt to the networks topological constraints. Despite greater difficulties such as much lower solubility for titanium phosphates compared to aluminium or gallium ones, this approach was successfully used.[46]

3.2.2 The microporous πTiP case. The *in* and *ex situ* study of the titanium phosphate πTiP or $Ti_2O(PO_4)_2{\cdot}2H_2O$ was performed. This latter compound was selected since it is synthetically related to a mesostructured hexagonal titanium fluorophosphate (see below). This solid is built up from dimers of titanium octahedra and phosphate groups resulting in a three-dimensional framework whereas seven-membered rings channels are present with a terminal water molecule pointing at the tunnels (see Fig. 4). Two different SBU are proposed for this solid, *i.e.* two different Ti_2P_2 4R units.

3.2.2.1 Primary building units. The first step of our methodology is to perform a preliminary study of the titanium fluoride and titanium fluorophosphate in water. Actually this is a mandatory step for NMR data concerning the fluorophosphate system are scarce. All the successive $TiF_x(H_2O)_{6-x}^{4-x}$ species were experimentally observed, confirming previously reported species, and for the first time the spectral signature of $TiOF(H_2O)_4^+$ was provided as well as equilibrium constants determined. Fluorophosphate complexes $TiF_x(H_3PO_4)_y(H_2O)_{6-x-y}^{4-x}$ were also observed, and several species containing fluorides and phosphates identified. Finally for titanium fluorophosphate system, almost all the successive complexes from "Ti^{4+}" to TiF_6^{2-} are observed with many of the

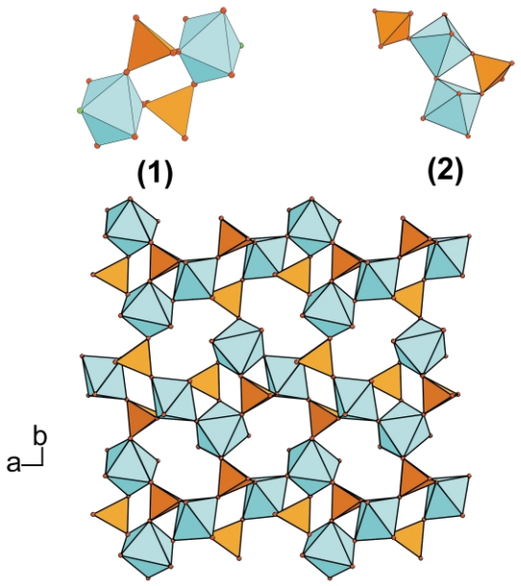

Fig. 4 Structure of TiP along the *c*-axis. The two possible PNBUs are represented at the top of the figure. Experimental data are consistent with **2**.

combinations of water substituted by phosphate to complete the coordination sphere at six.

The special role of the titanyl bond was also confirmed for the F/H_2O system with a dual regime, *i.e.* low fluorinated complexes with a titanyl bond coexisting with highly fluorinated complexes with no titanyl group. This regime was however not observed within the $F/P/H_2O$ system. Furthermore, it was pointed out that when adding phosphates to fluorides complexes in water, the exchange phenomenon between H_3PO_4 and H_2O in and out the coordination sphere is quenched. This is in contrast to aluminium fluorophosphate complexes, for which the in and out exchange takes place for all compositions. It is suggested that one H_2O and one H_3PO_4 in the titanium coordination sphere interact through an internal hydrogen bond, slowing down the in and out chemical exchange.

3.2.2.2 In situ NMR. The very low solubility of titanium phosphate in water was definitely a concern during this study. At pH = 0.5 (pH of synthesis), the solubility does not exceed 5.10^{-4} Mol l^{-1} at room temperature. Despite its weak value, an *in-situ* study of πTiP was performed. Both ^{19}F and ^{31}P NMR experiments showed two signals, with a 1 : 1 ratio, of chemical shifts −68.8 and −71.2 ppm (^{19}F) and −1.5 and −8.5 ppm (^{31}P) appearing after a few hours of synthesis at 150 °C (see Fig. 5). One must emphasise the care to take, to pin point these weak signals in the presence of many others due to interconverting PBU of much higher intensity. This remark applies to titanium fluorophosphates as it applies to silicon NMR which is obviously even less sensitive. Supersaturated species are delicate to observe.

For πTiP, two possible SBUs can be suggested by retrosynthesis analysis, from the crystallographic structure, both with a Ti_2P_2 stoichiometry (Fig. 4). First, two crystallographically equivalent titanium octahedra connected only *via* two crystallographically equivalent phosphate groups, in Q2 connectivity. Second, a titanium dimer, with two inequivalent titanium atoms, connected to two inequivalent phosphate groups, one bridging the two titanium atoms and the other one being a terminal group connected to only one titanium atom, of respectively Q2 and Q1 connectivity. At first, one might have chosen the four-ring (4R) unit considering that it seems to be a

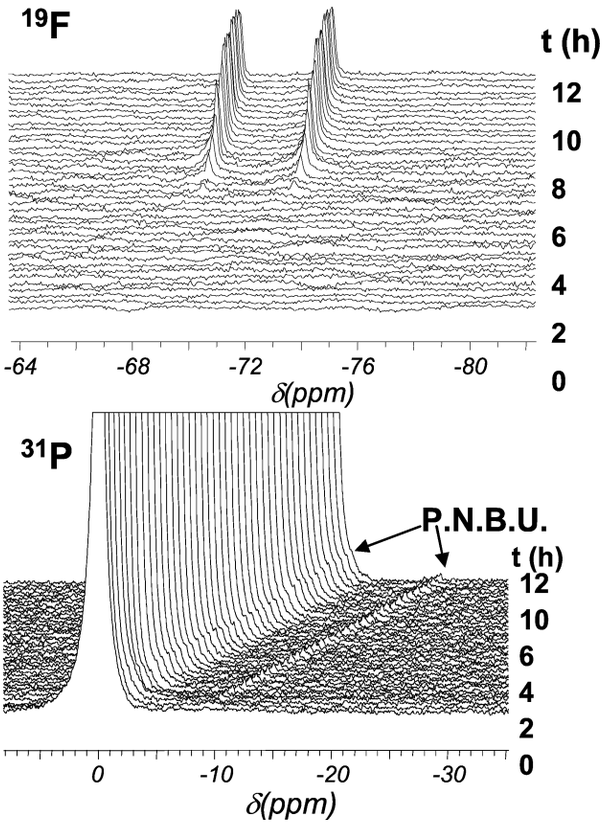

Fig. 5 *In situ* ^{31}P liquid NMR spectra as a function of time for πTiP at 150 °C. (Top): ^{19}F NMR (Bottom) ^{31}P NMR.

general condensation scheme for zeolite as well as AlPO materials for high density charge amine.[20,47] However, considering the chemical shifts observed during ^{31}P *in situ* NMR experiments ($\delta \approx -1.5$ and −8 ppm) and those observed during previous ^{31}P liquid NMR experiments of solutions of titanium phosphates, a difference of 7 ppm correspond to a change in metal–phosphorus connectivity. This rules out the 4R type of SBU. The PNBU is built up from a titanium dimer with two non-equivalent phosphate groups in asymmetric positions. This result is consistent with the formation of a Ti–O–Ti bond vertex connection between two TiO_6. On the ^{19}F side, two inequivalent signals are observed. Two possibilities exist. The two fluorine are either located on the same titanium atom or on two different titanium atoms. No J_{F-F} coupling is observed indicating that the two fluorine sites are not on the same titanium atom, but J_{F-F} could have been unresolved in the lineshape. A ^{19}F COSY NMR experiment, performed at room temperature, using an *ex situ* supernatant liquid obtained after fifteen hours of synthesis of πTiP at 150 °C, shows that the two fluorine are neither J_{F-F} coupled nor at small dipolar distance. One can therefore conclude that PNBU is a dimer of titanium octahedra grafted with two phosphate groups of Q1 and Q2 connectivity and with one fluorine per titanium (Fig. 6).

3.2.2.3 Ex situ study. Synthesis at 150 °C of πTiP was stopped at times between 0 and 45 hours. Each time, the supernatant and the solid were separated and analysed by NMR, in liquid or solid conditions. Additionally, X-ray powder diffraction and quantitative analysis were made also on the solid fraction.

The liquid NMR results are presented first. Under our conditions, HF, titanium fluorides and titanium fluorophosphate monomeric species are present in solution. ^{19}F experiments are

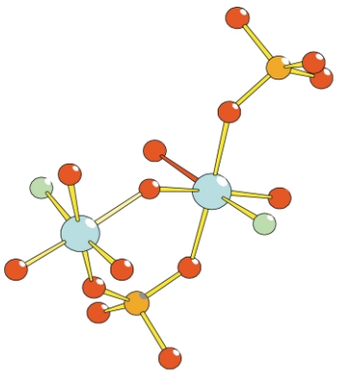

Fig. 6 Proposed structure of the PNBU involved in the crystallisation of πTiP. Titanium, phosphorus and fluorine, atoms are in cyan, orange, green , respectively.

much better resolved than ^{31}P spectra. The evolution of integrated NMR signals is displayed on Fig. 7. A global

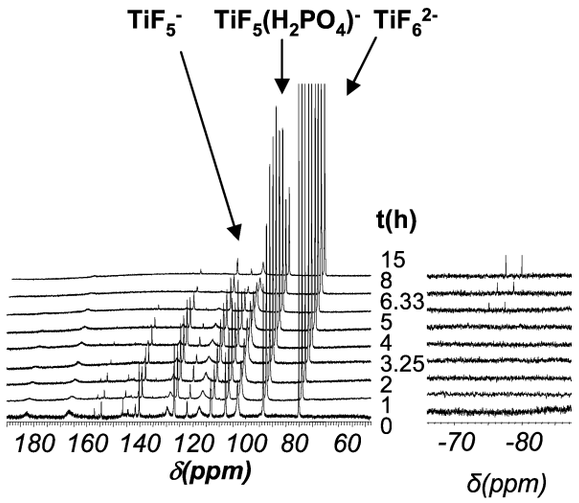

Fig. 7 *Ex situ* ^{31}P liquid NMR spectra of πTiP as a function of time. The negative part of the spectra has been enlarged (*100) for a better understanding.

decrease of the fluorophosphate complexes and an increase in HF occurs during the synthesis. Some species ($TiF_5(H_2PO_4)^{2-}$) exhibit a peculiar behaviour (Fig. 8), increasing first then decreasing at the end of the synthesis. The PNBU signals appear after a few hours and their intensity increases with time. The total amount of fluorine in solution increases with time, in agreement with precipitation of a non-fluorinated titanium phosphate.

Titanium fluorophosphate complexes disappear during the first eight hours of the synthesis, releasing HF in solution, changing the TiF_x^{4-x} distribution in favour of highly fluorinated titanium species. After eight hours, fluorophosphates are no longer consumed and the concentration of titanium fluorides decreases slightly with time. From these results, two kinds of PBUs could be distinguished: "Passive PBUs" *i.e.* the highly fluorinated titanium fluorophosphates ($TiF_5(H_2PO_4)^{2-}$, $TiF_4(H_2PO_4)_2^{2-}$) whose concentration increases or remains stable during the first hours of the synthesis and decreases partially at the end (Fig. 8) and the "Reactive PBUs" *i.e.* the less fluorinated complexes ($TiF_3(H_2PO_4)_3^{2-}$, $TiF_2(H_2PO_4)_3^{-}$…), which are completely consumed during the first eight hours of the synthesis (Fig. 8). Finally, the concentration of the PNBU increases between 5 and 10 hours to reach a plateau at the end of the synthesis.

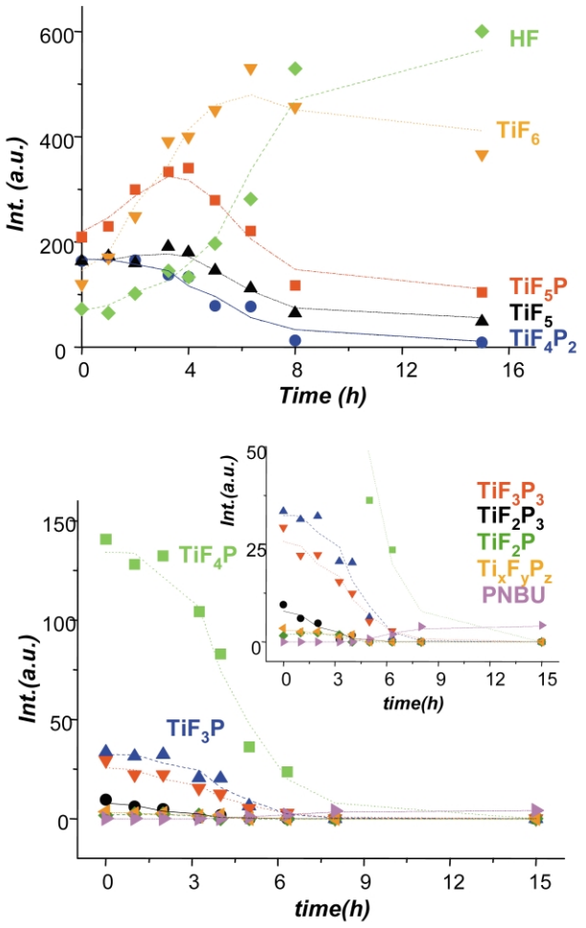

Fig. 8 Evolution of the relative concentration of the fluorinated complexes present in the liquid phase as a function of time during the synthesis of phase πTiP at 150 °C. (Top): the passive complexes. (Bottom): the reactive species; in the latter case, an enlargement is included at the top right of the figure. For a better understanding, only approached formula of the complexes are given.

In as second step, the *ex situ* study of the solid is performed for πTiP.[41] A precipitate does not appear before 3 hours. Both XRD and ^{31}P solid state NMR indicate that an intermediate phase, a layered titanium phosphate of unknown structure, denoted TiOP or $Ti_2O_3(H_2PO_4)_2{\cdot}2H_2O$, crystallises between 2 and 4 hours. After four hours, TiOP is consumed while the crystal growth of πTiP begins. The yield of the reaction reaches a 67% yield in titanium after 15 hours and quantitative analysis is consistent with a phase transformation of phase TiOP into πTiP, which is reminiscent of an analogue transformation in steps experienced during SAPO34 transformation equally followed by *in-situ* XRD and NMR.[48–50] The several steps of SAPO34 involved a progressive loss of fluoride of the PNBU and related structures.

3.2.3 Conclusion. A tentative structure of the PNBU, involved in the crystallisation of πTiP, has been proposed which is consistent with both the NMR observation in solution and the crystal structure. This PNBU is a tetrameric Ti_2P_2 unit built up from a dimer of titanium octahedra grafted by two phosphate groups and two terminal fluorine atoms. The qualitative evolution of the concentration of the PBUs within the solution as well as the crystallisation process of the solids during the synthesis, have been described. Based on these results, it is now possible to propose a qualitative description of the mechanism of formation of πTiP.

4 Application: study of the formation of a hexagonal mesostructured titanium phosphate

4.1 Introduction

Recently, mesotextured hexagonal titanium fluorophosphates with a semi-crystalline framework were reported by our group.[51] During the study of these solids, it appeared that these latter were related to the πTiP solid. The mesophase, denoted H–TiP, turns into πTiP when hydrothermally treated at temperatures higher than 120 °C, and this was the starting point of the study of the mesostructured solids using the *in-situ* and *ex-situ* methodology.[41]

4.2 *In* and *ex situ* study

4.2.1 *In situ* study. The ^{19}F and ^{31}P *in situ* NMR of H–TiP was first performed at 100 °C. In both cases, two very weak signals were visible after 1–2 hours and their intensities stabilise after 3–4 hours. They exhibit a 1 : 1 ratio, at −69.2 and −72.5 ppm (Fig. 9) for ^{19}F spectra and two weak signals at −2.0 and

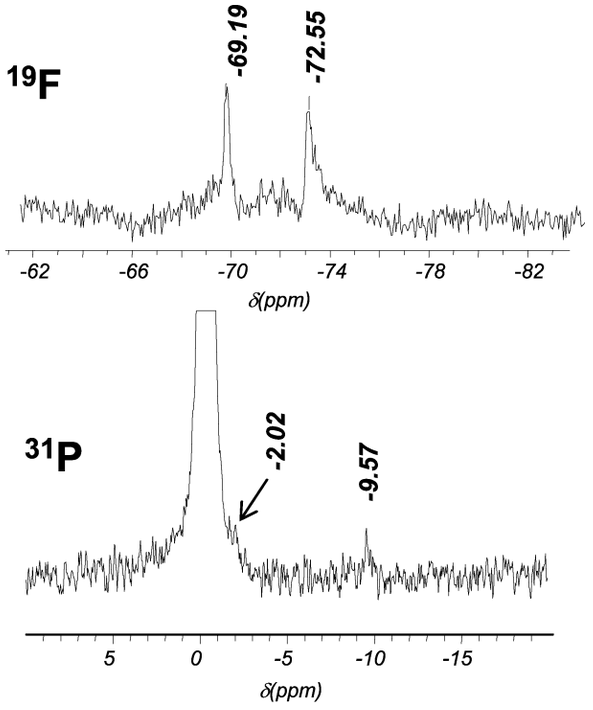

Fig. 9 *In situ* liquid NMR spectra performed at the end of the synthesis (15 h at 100 °C). Top: ^{19}F spectrum; Bottom: ^{31}P spectra.

−9.6 ppm for ^{31}P NMR at the limit of detection. Further experiments will confirm its existence (see *ex situ* results). They increase to reach a maximum after 9–10 hours.

Despite low signal to noise ratios, one must notice almost identical chemical shifts to the πTiP PNBU. This very important result indicates that crystallisations of πTiP and H–TiP occur probably through a common step involving the same PNBU.

4.2.2 *Ex situ* study. First, the evolution of the different species in solution has been followed using liquid ^{19}F and ^{31}P NMR study (Fig. 10). Again, two types of PBUs are present: the "passive PBUs" and the "reactive PBUs" (Fig. 10). The formation of H–TiP occurs in two steps: first, precipitation of a mesostructured solid at room temperature followed by an aging treatment. At room temperature, all "reactive" or "passive" PBUs are more or less consumed. This is consistent with the formation of fluorinated mesophase. During the first hours of hydrothermal aging, only the "reactive" PBUs, and the

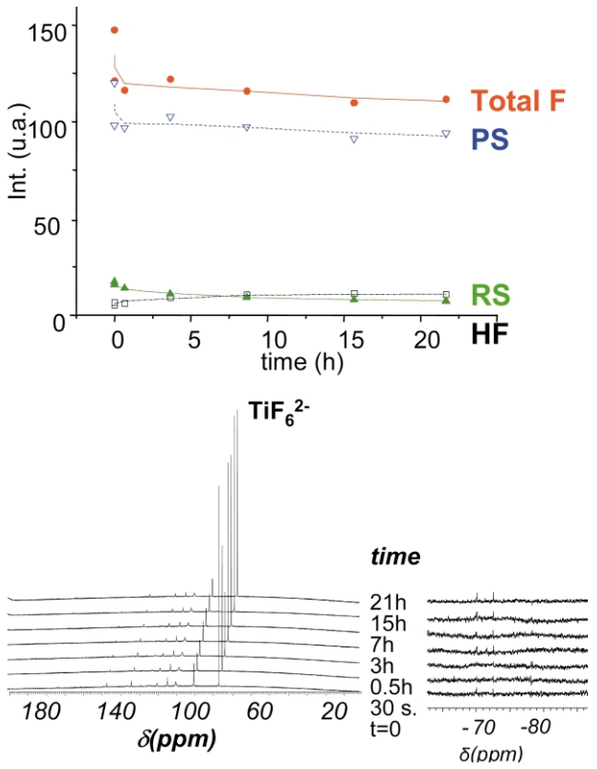

Fig. 10 (Above): *Ex situ* ^{19}F liquid NMR spectra of phase H as a function of time. (Below): Evolution of the relative concentration of the fluorinated PBUs, passive or reactive, present in the liquid phase as a function of time during the synthesis of phase H. The negative part of the spectra has been enlarged (*100) for clarity.

oligomeric complex $Ti_xF_y(H_2PO_4)_zX_n$), keep on being consumed (Fig. 10) while the concentration of the "passive" PBUs remains approximately stable and the concentration of HF slightly increases. The PNBU signals appear at −69 and −71.5 ppm during the aging period, and their intensity increases with time. After 10–15 hours, no evolution is observed in the liquid phase.

Then, the solid *ex situ* study of the formation of the mesophase. XRD, solid state NMR and quantitative analysis indicate (Fig. 11) that the initial solid formed at room temperature is a mesostructured solid with amorphous pore walls (see the broad ^{31}P NMR distribution) together with crystallised highly fluorinated surfactant salts (see ^{19}F results). During aging, NMR show that salts are dissolved and inorganic walls are crystallising. XRD indicates a crystalline Ti–P order within the walls (see reflection at 3.15 Å) while solid state NMR show distinguishable peaks both for ^{19}F and ^{31}P NMR, characteristic of an ordered solid. Finally, a quantitative analysis indicates that the crystallisation process uses reactive species with a constant stoichiometry, P : Ti=F : Ti ratio equal to 1, equivalent to those of the PNBU (Fig. 11).

4.3 Global approach of the mechanism of formation

A comparative description of the formation of the two titanium phosphates is proposed (Fig. 12). Starting from a mixture of PBUs in water, titanium complexes, fluorides and fluorophosphates, of monomeric or oligomeric structure, the presence of either small organic cations (TMA^+) or cationic micelles (CTAB) leads to two different structures. At first sight no direct relationship between the two solids: a three-dimensional hydrated titanium phosphate (πTiP) and a mesostructured solid, H–TiP. The formation of the two solids follows a similar route: precipitation of an intermediate solid which redissolves at the expense of the crystallisation of the final phase. In the case of

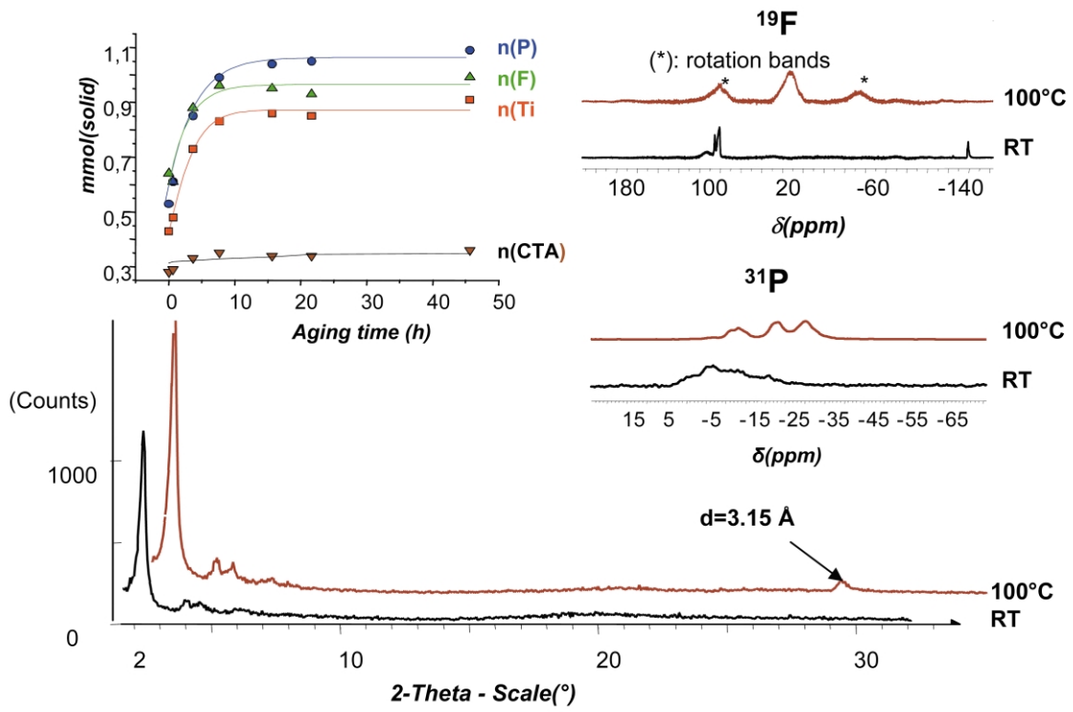

Fig. 11 Solid *ex situ* study of the formation of H–TiP. (Bottom): XRD pattern; (Right): Solid State NMR; (Top left): Number of moles of each component (Ti, F, P, CTA) as a function of time. RT: before aging at room temperature, 100 °C: aging period (15 hours) at 100 °C.

πTiP, the condensation of inorganic species occurs during the first hours of the synthesis, followed by a precipitation of an intermediate solid, a hydrated titanium phosphate with a layered structure (TiOP), which redissolves to produce πTiP. Based on other results concerning the *in situ* study of the crystallisation of SAPO-34,[48–50] the PNBU involved in the crystallisation of the intermediate phase TiOP is probably closely related to those of the final solid πTiP, and differs only by fluorine content.

H–TiP is formed in two steps: first, at room temperature, a hexagonal mesotextured solid with amorphous inorganic walls precipitates together with highly fluorinated crystalline surfactant salts. Aging (100 °C) leads to crystallisation of the walls and dissolution of the salts. Further aging at temperature above 120 °C leads eventually to the dissolution of the mesotextured solid to produce TiOP and then πTiP. In both cases, two types of PBUs are present in solution: "reactive" and "passive". The reactive PBUs are totally consumed during the crystallisation of the solid while the passive PBUs are only partially consumed or even generated upon the synthesis.

In both cases, reactive PBUs turn into a PNBU, of proposed formula $Ti_2OF_2(HPO_4)(H_2PO_4)X_5$ (X = OH, H_2O), which crystallises. The final connection of the PNBU to produce the solid is however different since no template is present for πTiP and micelles of surfactant are located within the pores in the case of the mesophase. In both cases, the PNBU is associated in solution with a counterion, TMA^+ or CTA^+, to create neutral pairs that eventually condense. This part of the mechanism of formation has still to be elucidated. However, by analogy with the crystallisation of SAPO-34,[49] the successive solids involved in the process are formed with a four ring PNBU that changes its fluorination state at each stage of the synthesis. As the fluorides protecting the functionality of titanium are progressively removed, the intermediate phases show an increasing dimensionality.

5 Conclusion

Despite a low solubility and the absence of titanium NMR, due to its low sensitivity, the mechanism of formation of an hexagonal mesostructured titanium fluorophosphate and a microporous titanium phosphate have been proposed, and, it appears that the PNBUs involved in both crystallisation processes are identical. This confirms the strong relationship between the two phases.

The *ex situ* study, confirmed the existence of the PNBU and allowed the monitoring of the concentration of the fluorinated and phosphated complexes during the synthesis. This is the basis of the qualitative description of both formation mechanisms. Finally, these results indicate that our investigation methodology is also successful for the formation of mesoporous compounds.

5.1 Open framework gallophosphates

During the past decade, the search for novel open framework fluorinated gallo- and alumino-phosphates has led to a wide range of structural types containing a limited number of SBU. This was the driving force to study the mechanism of formation of these materials since a relationship between the SBU and the reactive species responsible for the formation of the solid was expected. The first result concerned the aluminophosphate $AlPO_4$-CJ2 where for the first time the PNBU was characterised and identified as an isomer of the SBU of the solid. This method was furthered to study other solids such as ULM-3 and ULM-4 for which a PNBU was proposed,[52] this latter being again closely related to the SBU by isomerisation. This confirms that one PNBU leads to several two or three-dimensional solids (see Fig. 13) depending on the neutral pair PNBU-organic counterion, the number of associations being finite.[53]

Despite much more difficult NMR acquisition conditions, such as very low solubility, and with a lower number of characterised solids for titanium solids, the results presented here on titano-phosphates compare well with alumino- and gallo-phosphates. One observes the existence of passive and reactive PBUs, these latter condense in a PNBU and eventually form the solid through a precipitation dissolution followed by recrystallization mechanism process. However, some differ-

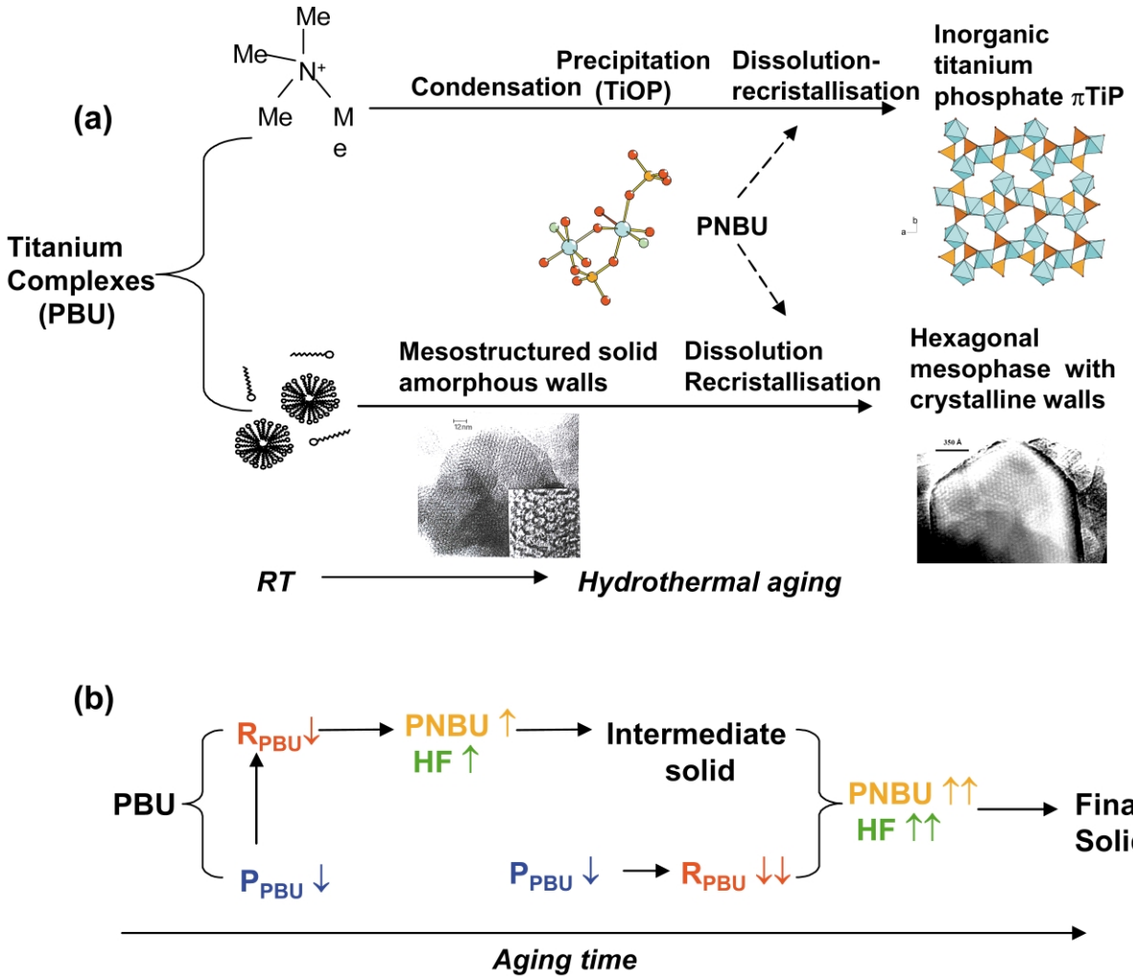

Fig. 12 (a) Schematic and comparative global approach of the mechanism of formation of πTiP and H–TiP. PBUs are titanium fluorides ($TiOF^{+}$, TiF_5^{-}, TiF_6^{2-}…) and fluorophosphates ($TiF_5(H_2PO_4)^{2-}$, $TiF_4(H_2PO_4)_2^{2-}$…); (b): General and qualitative evolution of the titanium species present in the liquid phase upon aging time during the synthesis of πTiP and H–TiP (R_{PBU}, P_{PBU}: reactive, passive PBU; PNBU: Pre-Nucleation Building Units).

ences can be pointed out. The key difference is the lower number of possible PNBUs for the titanium system. Firstly, changing from a trivalent to a tetravalent cation leads to the formation of higher charged oligomers which limits the range of charge density of the possible PNBU. Secondly, fluorine which can be found as terminal or bridging anion in the alumino or gallophosphates is encountered only in a terminal position in the titanium(IV) phosphates. It acts only as a reducer of the titanium connections. There are therefore fewer possibilities for creating new topologies for a given PNBU. Finally, the NMR study has provided some new data on the titanium chemistry in water. In the presence of fluorine and phosphates, the titanium(IV) chemistry in water is first governed by the acidity of the first acidic solution. The hydrolysis ratio of Ti governs the number of Ti–O–Ti bond formation. The competitive complexation of titanium by fluorine and phosphates controls the functionality of titanium, fluorine protecting titanium(IV) from further networking connection, and the final pH ratio controls, *via* deprotonation of phosphate groups, the dimensionality of the crystal.

5.2 Outlook

The methodology developed to analyse hydrothermal syntheses of fluorinated alumino and gallophosphates open frameworks, using *in-situ* and *ex-situ* NMR and XRD, has been applied successfully to the titanium system. The results obtained for the study of a micro- and a mesoporous solids show a general method for elucidating all the different chemical steps of the fluorometallophosphates crystal tectonics. Every component of the reactive species plays more than one role but the plot of the play can be unveiled.

This method opens the way to syntheses of new materials. Instead of following the usual "trial and error" strategy, a crystal with a known SBU, as it dissolves in its corresponding PNBU could be used as the source to generate other crystals. Such a strategy has been claimed by Ozin.[54] Rao[55] and coworkers on zinc and tin phosphates used the amine phosphates route. It has been used by Lillerud[49] by profiling the temperature in order to redissolve the low temperature phase that is followed by formation of SAPO34.

Design of hybrid inorganic–organic microporous solids has meanwhile been developed by O'Keeffe and Yaghi using inorganic tetramers with divalent cations (Zn, Cu…) and organic linkers such as dicarboxylates to create tailored made porous solids.[56] Finally, for "traditional" zeolites or nanoporous metallophosphates, designing new materials is still needed and our method allows elucidation in each case of the parameters that control the different facets of the rational design of such materials. Even if there are still some technical limitations, especially in the realm of NMR sensitivity, the methodology is general and will benefit from all the current technical developments in NMR, with especially higher magnetic field and better detection methods.

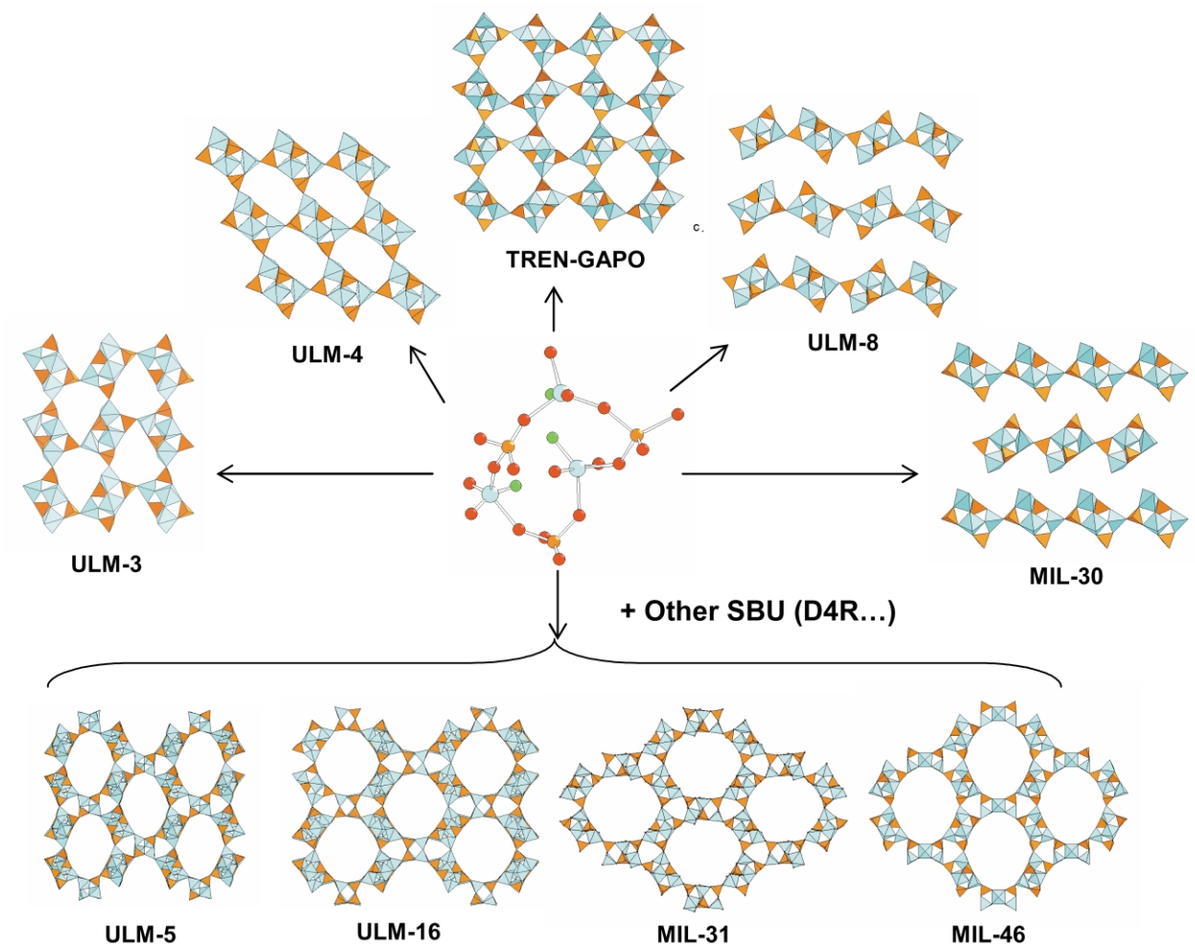

Fig. 13 Inventory of the open framework gallophosphates exhibiting an hexameric unit as one of its SBUs. The central ball and sticks hexamer is a representation of the PNBU proposed for the synthesis of ULM-3 and ULM-4 solids; gallium, phosphorus, oxygen, fluorine atoms are represented in cyan, orange, red and green respectively. For a better understanding, water and template molecules have been removed.

Lehn has developed the concept of supramolecular chemistry,[57] and a large community of molecular chemists is successfully building up all sorts of molecular objects by design. Along the same line molecular chemists, successfully design molecular networks, by molecular tectonics,[58] and some engineer crystals. To succeed performing rational design of crystals of nanoporous materials based on metallophosphate chemistry, we have presented a general strategy allowing acquisition of the basic knowledge necessary to control the different steps of crystal construction. For crystal construction, the main chemical steps have been identified. They are:

1. Generating the reactive function around the metal;
2. Protecting and unprotecting functions;
3. Activation of the function, here by pH;
4. Generation of definite entities (PNBU);
5. Polymerising in 1 to 3D;
6. Sequencing the construction through redissolution of crystals acting as the source for the following step.

Actually the whole toolbox that supramolecular chemists have been patiently and efficiently building in the kingdom of organic chemistry, is progressively transposed in the domain of inorganic materials, albeit at a cost, establishing a large body of facts concerning all the atoms of the Mendeleev table other than C, H, O, N. This work has already been initiated for sol–gel chemistry with essentially oxide/hydroxide formation,[14,16,17] but is now extended in the rational design of nanoporous materials with several chemical agents performing all the tasks required to achieve the scaled chemistry construction.

Notes and references

1 A. K. Cheetham, G. Férey and T. Loiseau, *Angew. Chem., Int. Ed. Engl.*, 1999, **38**, 3269.
2 S. Feng and R. Xu, *Acc. Chem. Res.*, 2001, **34**, 239.
3 G. Férey, *Chem. Mater.*, 2001, **13**, 3084.
4 A. Clearfield and J. A. Stynes, *J. Inorg. Nucl. Chem.*, 1964, **26**, 117.
5 S. F. Alluli, C. La Ginestra, M. A. Massucci and M. A. Tomassini, *J. Inorg. Nucl. Chem.*, 1977, **39**, 1043.
6 R. Masse, A. Durif and J. C. Guitel, *Z. Kristallogr.*, 1974, **139**, 103.
7 C. Delmas and A. Nadiri, *Solid State Ionics*, 1988, **28–30**, 419.
8 B. Notari, *Catal. Today*, 1993, **18**, 163.
9 J. S. Reddy, R. Kumar and P. Ratnasany, *Appl. Catal.*, 1990, **58**, 1.
10 T. Blasco, M. A. Cambor, A. Corma and J. Perez-Patiente, *J. Am. Chem. Soc.*, 1993, **115**, 11806.
11 J. S. Beck, J. C. Vartuli, W. J. Roth, M. Leonowicz, C. Kresge, K. Schmitt, C. T. Chu, D. Olson, E. Sheppard, M. Cullen, J. Higgins and J. L. Schenkler, *J. Am. Chem. Soc.*, 1992, **114**, 10834.
12 A. Corma, *Chem. Rev.*, 1997, **97**, 2373.
13 F. Schüth, *Chem. Mater.*, 2001, **13**, 3184.
14 M. Henry, Molecular Tectonics in Sol–Gel Chemistry, in *Handbook of Organic–Inorganic Hybrid Materials and Nanocomposites*, ed. H. S. Nalwa, American Scientific Publishers, California, 2003.

15 F. A. Cotton and G. Wilkinson, *Advanced Inorganic Chemistry*, John Wiley & Sons, 5th edition, New York, 1988.
16 J. P. Jolivet, *De la Solution a L'oxyde*, Intereditions/CNRS editions, Paris, 1994.
17 J. Livage, M. Henry and C. Sanchez, *Prog. Solid State Chem.*, 1988, **18**, 259.
18 C. C. Sanchez and J. Livage, *New J. Chem.*, 1990, **14**, 513.
19 F. Taulelle, M. Haouas, C. Gerardin, C. Estournes, T. Loiseau and G. Férey, *Colloids Surf., A*, 1999, **158**, 299.
20 F. Taulelle, M. Pruski, J. P. Amoureux, D. Lang, A. Bailly, C. Huguenard, M. Haouas, C. Gerardin, T. Loiseau and G. Férey, *J. Am. Chem. Soc.*, 1999, **121**, 12148.
21 F. Taulelle, *Solid State Sci.*, 2001, **3**, 795.
22 F. Taulelle, *Curr. Opin. Solid State Mater. Sci.*, 2001, **5**, 397.
23 G. Férey, *J. Fluorine Chem.*, 1995, **72**, 187.
24 G. Férey, *C. R. Acad. Sci.*, 1998, **1**, 1.
25 D. M. Poojary, A. I. Bortun, L. N. Bortun and A. Clearfield, *J. Solid State Chem.*, 1997, **132**, 213.
26 S. Ekambaram and S. C. Sevov, *Angew. Chem., Int. Ed. Engl.*, 1999, **38**, 372.
27 S. Ekambaram, C. Serre, G. Ferey and S. C. Sevov, *Chem. Mater.*, 2000, **4**, 380.
28 C. Serre and G. Férey, *C. R. Acad. Sci. serie IIc*, 1999, **2**, 147.
29 C. Serre and G. Férey, *Inorg. Chem.*, 1999, **38**, 5370.
30 C. Serre and G. Férey, *Inorg. Chem.*, 2001.
31 C. Serre and G. Férey, *J. Mater. Chem.*, 1999, **9**, 579.
32 C. Serre, F. Taulelle and G. Férey, *Chem. Mater.*, 2002, **14**, 998.
33 C. Serre, N. Guillou and G. Férey, *J. Mater. Chem.*, 1999, **9**, 1185.
34 Y. S. Liu, L. Zhang, Y. Fu, J. Chen, B. Li, J. Hua and W. Pang, *Chem. Mater.*, 2001.
35 Y. Zhao, G. Zhu, X. Jiao, W. Liu and W. Pang, *J. Mater. Chem.*, 2000, **10**, 463.
36 Y. Guo, Z. Shi, J. Yu, J. Wang, Y. Liu, N. Bai and W. Pang, *Chem. Mater.*, 2001, **13**, 203.
37 C. Serre, F. Taulelle and G. Férey, *Solid State Sci.*, 2001, **3**, 623.
38 C. Serre and G. Férey, *C. R. Acad. Sci. serie IIc*, 1999, **2**, 85.
39 M. Henry, J. P. Jolivet and J. Livage, in *Chemistry, Spectroscopy and Applications of Sol-Gel Glasses*, ed. R. R. a. C. K. Jorgensen, Berlin, 1992.
40 P. Comba and A. Merbach, *Inorg. Chem.*, 1987, **26**, 1315.
41 M. Henry, in *Pacha*, Strasbourg, 2003.
42 C. Serre, C. Lorentz, F. Taulelle and G. Férey, *Chem. Mater.*, 2002, **14**, 4939.
43 L. Ciavatta, *Polyhedron*, 1985, **4**, 15.
44 H. Stünzy and W. Marty, *Inorg. Chem.*, 1983, **22**, 2145.
45 C. E. A. Kirschhock, R. Ravishankar, L. Van Looveren, P. A. Jacobs and J. A. Martens, *J. Phys. Chem. B*, 1999, **103**, 4972.
46 C. Serre, C. Lorentz, F. Taulette and G. Férey, *Chem. Mater.*, 2003, **15**(12), 2328.
47 R. Walton and D. O'Hare, *Chem. Commun.*, 2000, 2283.
48 B. Vistad, D. E. Akporiaye and K. P. Lillerud, *J. Phys. Chem. B*, 2001, **105**, 12437.
49 O. B. Vistad, D. E. Akporiaye, F. Taulelle and K. P. Lillerud, *Chem. Mater.*, 2003, **15**, 1639.
50 O. B. Vistad, D. E. Akporiaye, F. Taulelle and K. P. Lillerud, *Chem. Mater.*, 2003, **15**, 1650.
51 C. Serre, M. Hervieu, C. Magnier, F. Taulelle and G. Férey, *Chem. Mater.*, 2002, **14**, 180.
52 M. Haouas, NMR study of the hydrothermal synthesis of oxyfluorinated microporous aluminophosphates: $AlPO_4$-CJ2, ULM-3 and ULM-4, Thesis of the University of Strasbourg, Strasbourg, France, 1999.
53 C. Sassoye, J. Marrot, T. Loiseau and G. Férey, *Chem. Mater*, 2002, **14**, 1340.
54 S. Oliver, A. Kuperman and G. A. Ozin, *Angew. Chem., Int. Ed.*, 1998, **37**, 46.
55 C. N. R. Rao, S. Natarajan, A. Choudhury, S. Neeraj and A. A. Ayi, *Acc. Chem. Res*, 2001, **34**, 80.
56 M. Eddaoudi, D. B. Moler, H. Li, B. Chen, T. Reineke, M. O'Keeffe and O. M. Yaghi, *Acc. Chem. Res*, 2001, **34**, 319.
57 J. M. Lehn, *Angew. Chem., Int. Ed.*, 1990, **102**, 1347.
58 J. Martz, E. Graf, M. W. Hosseini, A. De Cian and J. Fischer, *J. Mater. Chem.*, 1998, **8**, 2331.